

1 **An extremely large-volume, long-runout rock avalanche in the Trans Alai Ranges, Pamir**
2 **Mountains, Southern Kyrgyzstan.**

3
4 Tom R. **ROBINSON**, Tim R. H. **DAVIES**, Natalya V. **REZNICHENKO***, Gregory P. **DE**
5 **PASCALE**

6
7 Affiliation: University of Canterbury

8 Address: Department of Geological Sciences, University of Canterbury, Private Bag 4800,
9 Christchurch 8140, New Zealand

10 *Department of Geography, Durham University, South Road, Durham, DH1 3LE, UK

11 Corresponding author contact details:

12 E-mail: tom.robinson@pg.canterbury.ac.nz Tel: +64 3 364 2700 Fax: +64 3 364 2769

13
14 **Abstract**

15 Massive rock avalanche events form some of the most extensive landslide deposits on Earth and are
16 major geohazards in high-relief mountains. Recent reinterpretation of previously-reported glacial
17 deposits in the Alai Valley of Kyrgyzstan identified a large volume, long-runout rock avalanche
18 deposit in the Komansu River catchment. This deposit likely covers an area $\sim 100 \text{ km}^2$, has a
19 minimum volume of 10 km^3 and a runout of $\sim 28 \text{ km}$. This makes it the longest-runout, and one of the
20 largest-volume, subaerial non-volcanic rock avalanches thus far identified on Earth. The event
21 appears to have occurred 5000-11000 yr B.P., possibly when the region's glaciers were further
22 advanced. It originated in the Trans Alai ranges and we identify a likely source zone within the
23 ranges. Runout appears to have halted when the debris reached the foothills of the Tien Shan at the
24 northern extent of the Alai valley where the deposit ran uphill about 100 m requiring a minimum
25 velocity of 45 m s^{-1} . The rock avalanche was most likely initiated by a large-to-great (M7-M8)
26 earthquake on the range-bounding Main Pamir Thrust, which is known to have sustained similar
27 earthquakes in recent history. The deposit length suggests an apparent coefficient of friction during
28 runout of ~ 0.11 , much smaller than 'normal' apparent coefficient of frictions of >0.6 . This may have
29 resulted from partial runout over glacial ice; however the apparent friction is expected empirically
30 for events of this volume even in the absence of ice. Sedimentary evidence for intense basal
31 fragmentation was found suggesting a likely mechanism for the reduced friction coefficient.

32
33 **Keywords**

34 **Rock avalanche; long-runout; dynamic fragmentation; glacial deposits; coefficient of friction**

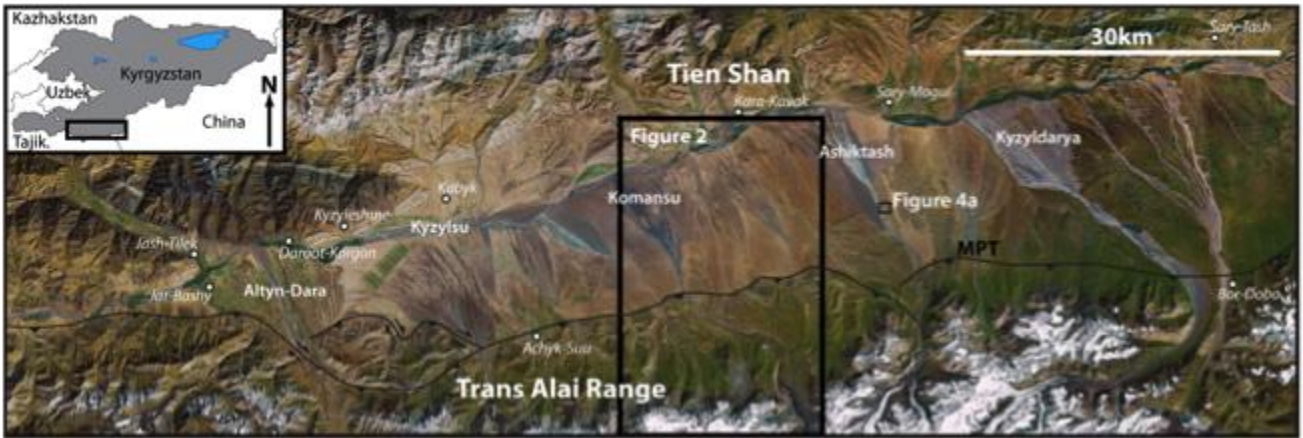
35 **Introduction**

36 Large ($>10^6$ m³) rock avalanches with unusually long run-out distances (up to tens of kilometres)
37 occur infrequently in mountain ranges and from volcanic edifices. Rock avalanche deposits have
38 been identified at numerous locations on Earth as well as on Mars and the Moon (e.g. Lucchitta,
39 1978; Quantin et al., 2004; Lucas and Mangeney, 2007). Their deposits sometimes bear a striking
40 morphometric resemblance to glacial deposits often resulting in misinterpretation: for example, re-
41 examination of deposits in the Karakoram Himalayas by Hewitt (1999) resulted in 15 previously-
42 reported glacial deposits being re-interpreted as rock avalanche deposits. Similar re-interpretations
43 have also occurred elsewhere (e.g. McColl and Davies, 2010; Barth, 2013). Incorrectly identifying
44 rock avalanche deposits as glacial deposits can result in underestimated geohazards risk (McColl and
45 Davies, 2010), whilst also contaminating regional paleoclimate reconstructions vital for
46 understanding of global climate dynamics.

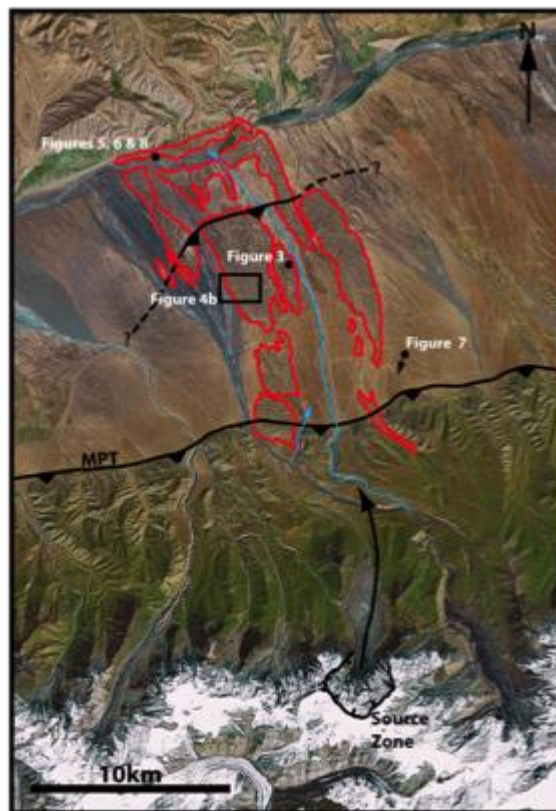
47 Large rock avalanches are typically characterised by high mobility resulting in unusually small
48 apparent coefficients of friction ($=H/L$; where H is the total fall height and L is the total travel
49 distance) of <0.6 (Hsü, 1975). Several explanations for this apparent reduction of friction have been
50 proposed including air cushioning (Shreve, 1966), acoustic fluidisation (Melosh, 1979), mechanical
51 fluidisation (Davies, 1982), and lubrication from molten basal layers (Erismann, 1979). However,
52 currently none of these explanations are generally accepted within the scientific community (Davies
53 and McSaveney, 2012). Rock avalanches can be triggered by a number of different factors including
54 strong ground motions during large earthquakes, volcanic eruptions, heavy or long-duration rainfall,
55 rapid snow melt, or a combination of these. In addition, some appear to have no definitive trigger
56 (e.g. Sigurdsson and Williams, 1991; McSaveney, 2002; Hauser, 2002). Identifying the cause of a
57 prehistoric event is therefore difficult; however, analysis of the local and regional environment as
58 well as estimates of the timing of the event can provide some insights. Analysis of the deposit
59 morphology and of the internal structure, if exposed, can offer understanding of the emplacement
60 dynamics.

61 The intramontane Alai Valley in the Northern Pamir Mountains of Kyrgyzstan (Fig. 1) has numerous
62 large-scale deposits previously interpreted as glacial moraines (e.g. Nikonov et al., 1983;
63 Arrowsmith and Strecker, 1999; Strecker et al., 2003). However, recent analysis by Reznichenko et
64 al. (2013) re-evaluated one of these deposits and determined that in fact it is a rock avalanche
65 deposit. This deposit, on the true right of the Komansu River (Fig. 2), extends north 28 km from the
66 Trans Alai ranges of the Pamir Mountains to the foothills of the Tien Shan Mountains (Fig. 2),
67 making it one of the longest-runout subaerial rock avalanche deposits identified on Earth. Only the

68 distal half of the deposit is exposed at the surface, and this covers an area ~100 km² with the
 69 proximal section of the deposit missing (Fig. 2).
 70 This study aims to answer specific questions about the Komansu rock avalanche event including the
 71 failure mechanism and the dynamic processes involved in the runout of the rock avalanche. This
 72 analysis is based on field studies and the interpretation of aerial and satellite images. We also discuss
 73 the implications for hazard analysis of such events.



74
 75 **Fig 1 Satellite image of the Alai Valley showing the major towns, rivers, mountain ranges within the**
 76 **region. MPT – Main Pamir Thrust. Boxes indicate areas shown in Figures 2 & 4a**



77
 78 **Fig 2 Komansu River catchment showing the exposed Komansu rock avalanche deposit, with probable**
 79 **source headscarp and runout path. Black lines show fault scarps; MPT – Main Pamir Thrust; black**

80 arrow shows likely runout path; red lines show surficial exposure of the deposit; blue lines show the
81 inferred position of the Komansu River immediately after the event (see text); black circles show
82 location of figures. Box indicates area shown in Figure 4b

83

84 **Regional Setting**

85 *Tectonics*

86 The Komansu deposit lies in the centre of the Alai Valley in southern Kyrgyzstan, between the Pamir
87 and Tien Shan Mountains (Fig. 1). The Alai Valley separates the Trans Alai (also known as Zaalai)
88 range of the Northern Pamir from the Tien Shan and was formerly part of a contiguous Cenozoic
89 sedimentary basin, connecting the Tajik depression in the west with the Tarim basin in the east
90 (Strecker et al, 2003). The Trans Alai range, which makes up the southern boundary of the Alai
91 Valley, formed as a result of Eurasian crust being over-thrust by the Pamir block during the late
92 Oligocene-early Miocene (Burtman and Molnar, 1993; Coutand et al., 2002) due to the Indo-
93 Eurasian collision to the south. As a result, the Trans Alai range reach elevations over 7000 m with
94 3000-3500 m of relief. The range is composed mainly of amalgamated and heavily deformed
95 Paleozoic and Mesozoic terrains while the Alai Valley consists primarily of large Quaternary alluvial
96 fans, moraines, and landslide deposits (Arrowsmith and Strecker, 1999). North of the valley, the Tien
97 Shan rise to over 5000 m with 2000-2500 m relief and is characterised by Devonian limestones and
98 Carboniferous metasediments overlain by Jurassic conglomerates and sandstones (Strecker et al.,
99 2003).

100 Present uplift of the Trans Alai range estimated from repeated GPS measurements is 15-30 mm yr⁻¹
101 (Burtman and Molnar, 1993; Arrowsmith and Strecker, 1999) which accounts for between 1/3 and 2/3
102 of the Indo-Eurasian Plate collision deformation at this location. Most of this shortening is thought to
103 occur along the range-bounding Main Pamir Thrust (MPT; Figs. 1 & 2). Arrowsmith and Strecker
104 (1999) estimated that uplift along this fault must be *at least* 6 mm yr⁻¹ based on geologic
105 observations while Krumbiegel et al. (2011) estimate a rate of 13 mm yr⁻¹ based on geodetic
106 observations. These rapid rates of convergence are supported by the high seismicity along the MPT
107 with several recent major earthquakes along the fault including M7.4 in 1949; M7.3 in 1974
108 (Zubovich et al, 2009); M6.5 in 1978 (Fan et al, 1994) and M6.7 in 2008 (Zubovich et al, 2009;
109 Krumbiegel et al, 2011).

110

111 *Quaternary History*

112 Due to the remote location and high elevation relatively limited research has previously been
113 undertaken in the area, resulting in a incomplete Quaternary history. Nevertheless, recent work by

114 Shatravin (2000) used oxide/proxide ratios of alluvial and proluvial deposits and proposed that the
115 last maximum glacial extent occurred 30,000 years before present (yr B.P.) with a smaller Holocene
116 re-advance around 8,000 yr B.P. According to Arrowsmith and Strecker (1999) and Shatravin (2000)
117 the period between the Pleistocene glacial maximum and the Holocene re-advance is represented in
118 the geologic record by numerous large landslide deposits. These deposits consist mainly of Neogene
119 sandstones and argillites sourced from the Trans Alai range and typically have a hummocky
120 topography and corresponding arcuate break-off scars (Arrowsmith and Strecker, 1999). Arrowsmith
121 and Strecker (1999) suggested that the largest of these had a runout of 5-6 km from the mountain
122 front.

123

124 **Geomorphology and Sedimentology**

125 Our re-interpretation of the Komansu deposit as a rock avalanche event is the result of detailed
126 ground investigations including analysis of the geomorphology as well as the sedimentology of the
127 deposit (Reznichenko et al, 2013). Below we provide a brief summary of the evidence for a rock
128 avalanche origin.

129

130 Surface Morphology

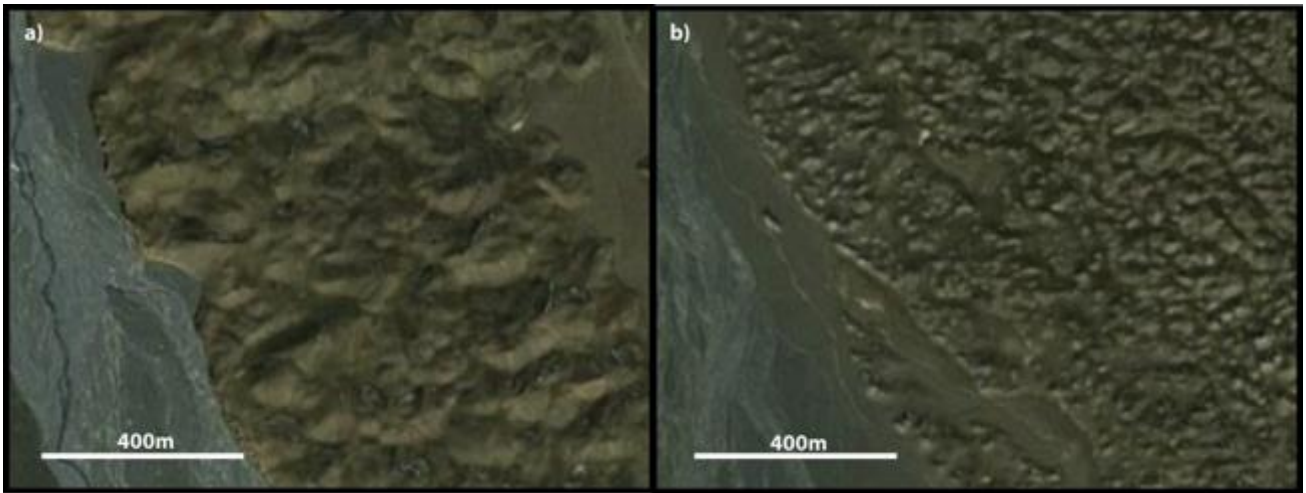
131 The Komansu deposit is clearly distinguishable from the surrounding alluvial deposits by its
132 pronounced hummocky terrain (Fig 3). These hummocks are small conical hills, >20 m in height and
133 50-60 m in diameter (Fig. 3). Arrowsmith and Strecker (1999) described hummocky topography as
134 being present in both glacial and landslide deposits within the Alai Valley, and such hummocks have
135 been identified in other large rock avalanche deposits including those at Socompa, in South America
136 (Wadge et al, 1995) and Fernpass in the European Alps (Prager et al., 2006) amongst others.
137 Hummocky terrain in the rock avalanche deposit from Round Top in New Zealand is thought to have
138 resulted from runout over outwash surface (Dufresne et al., 2010) which would also have occurred
139 during the Komansu event. Nevertheless, hummocks are not definitive evidence of rock avalanches
140 because they can also be characteristic of moraines, and thus Arrowsmith and Strecker (1999)
141 interpreted the Komansu deposit as of glacial origin. However, in the Alai Valley glacial hummocks
142 are typically larger than those of the Komansu deposit and interspersed with kettle-hole deposits
143 formed during glacial melt-out, none of which have been identified in the Komansu deposit
144 (Reznichenko et al, 2013). Figure 4 shows a comparison of the larger, chaotic hummocks of the
145 Ashiktash catchment glacial deposit ~20 km east of the study area and the smaller, more uniform
146 hummocks of the Komansu rock avalanche deposit.



147

148

Fig 3 Hummocky terrain of the Komansu deposit. View looking SW (see Fig. 2 for location).



149

150

151

Fig 4 Comparison of hummocks from the a) Ashiktash moraine deposit and b) Komansu rock avalanche deposit. Images from Google Earth.

152

153

Sedimentology

154

155

156

157

158

159

160

161

162

163

Clast counts were undertaken at several locations on the Komansu rock avalanche deposit in order to characterise lithology, clast size and roundness in an attempt to infer its likely origin. The deposit is dominated by angular to very angular and occasionally sub-rounded argillite and quartzite clasts of fine pebble to boulder size, in a matrix of very much finer material. These sediment characteristics correspond to reported descriptions of rock avalanche deposits which comprise a fragmented mass of angular to very angular clasts of the source lithology. Hewitt (1999) used this description to identify 15 rock avalanche deposits in the Karakorum Himalayas previously identified as moraines. The mainly argillite composition of the Komansu deposit agrees with the observation of Arrowsmith and Strecker (1999) of the lithologic composition of several other landslide deposits in the region whose sources are also in the Trans Alai range.

164

165

166

Reznichenko et al. (2012) developed a method to identify sediment of rock avalanche origin by the presence of characteristic micron-scale agglomerates, of widely-graded, largely subangular sub-micron clasts of parent material lithologies as observed under a Scanning Electron Microscope

167 (SEM). These agglomerates are the result of intense comminution of intact rock and rebonding of the
168 smallest fragments, under rapid, high-stress conditions during rock avalanche runout, and are absent
169 from sediments produced in lower stress and strain-rate glacial processes. Samples from the
170 Komansu deposit were shown by Reznichenko et al. (2013) to contain micron scale agglomerates
171 and hence they deduced a rock avalanche origin, confirming our sedimentologic and morphologic
172 deduction.

173

174 Basal Contact

175 The Kyzylsu River, which runs east-west through the Alai Valley (Fig. 2), has eroded through the
176 distal end of the deposit and exposed a long basal contact (Fig. 5). This sharp unconformity separates
177 the rock avalanche body from the alluvial terrace deposits beneath. At the eastern extent of the
178 outcrop the contact curves upwards before flattening out, thinning the rock avalanche deposit (Fig.
179 6a). Bedding in the underlying alluvium is clearly truncated against this contact (Fig. 6b) and we
180 interpret this as an ancient Kyzylsu River terrace which was over-ridden and partly preserved by the
181 rock avalanche.



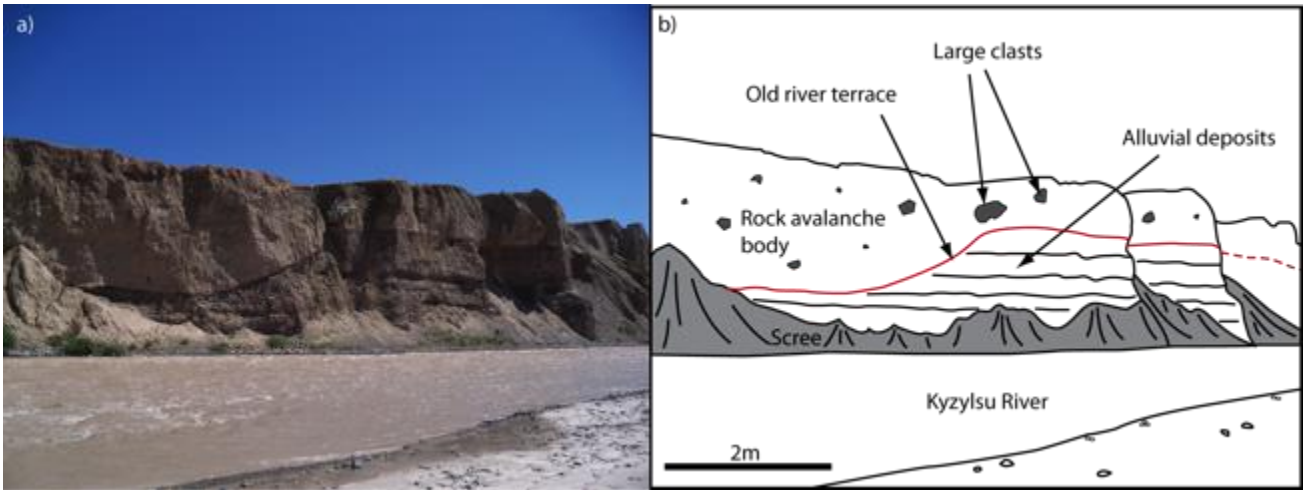
182

183 **Fig 5 Basal contact between Komansu rock avalanche deposit and alluvial deposits. View looking north**
184 **(see Fig 2 for location).**

185

186 Overlying Units

187 Overlying the rock avalanche deposit is a variable cover of fine-grained loess with thickness from
188 tens of centimetres to several metres. However, most of the loess and characteristic hummocks in the
189 central section of the deposit have been eroded away, corresponding with the location of an
190 abandoned river course (Fig. 2). Here the overlying deposits consist of alluvial sediments similar to
191 those beneath the rock avalanche deposit in figure 5. It is inferred that after the rock avalanche
192 deposit was emplaced, the Komansu River flowed through the centre of the deposit, eroding it and
193 depositing alluvial sediments. Subsequently the river has changed course to its present position on
194 the western flank of the deposit where it incised during uplift along the MPT into its present canyon.



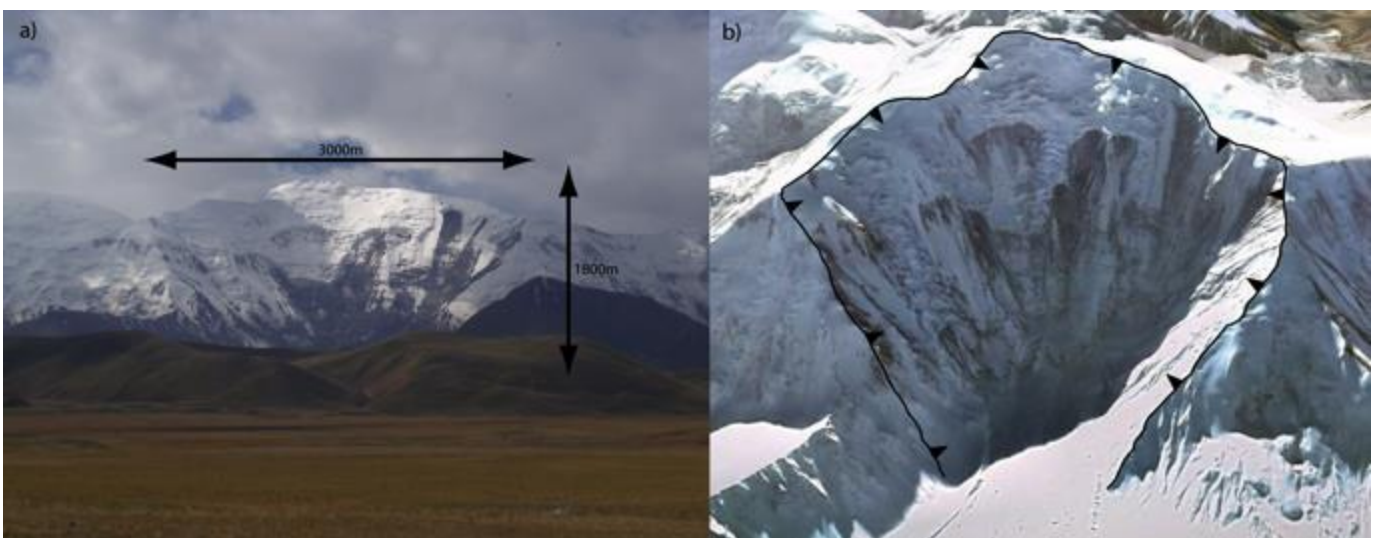
195
 196 **Fig 6 a) View of rock avalanche basal contact with underlying alluvial deposits, looking NE (see Fig 2**
 197 **for location); b) Interpretation. Red line shows position of basal contact.**

198

199 **Controlling Factors**

200 **Source Zone**

201 The location and extent of the Komansu deposit suggest that the rock avalanche has a source zone in
 202 the Trans Alai range to the south, rather than from the Tien Shan to the north (Fig. 2). The Trans Alai
 203 ranges are >7000 m high, and contain numerous glaciers. As a result we could not definitively
 204 identify the source zone. Nevertheless, far-field observation of the mountain range combined with
 205 satellite images and field mapping allowed us to identify a probable source zone (Figs. 2 & 7). This
 206 source zone shows the arcuate bowl shape typical of a large rock avalanche source (Turnbull &
 207 Davies, 2006), a sufficiently large size to yield the apparent volume of the deposit, and is suitably
 208 orientated to generate a landslide deposit in the same location as the current Komansu rock
 209 avalanche deposit (Fig. 2).



210

211 **Fig 7 a) Photograph looking SW at the probable source zone for the Komansu rock avalanche deposit**
212 **with dimensions (see Fig 2 for location); b) Google Earth image (looking SE) of the probable source**
213 **zone showing the detachment scar. Another large scar 8 km farther east is less well situated with**
214 **respect to the deposit so was discounted.**

215

216 Timing

217 Arrowsmith and Strecker (1999) suggested that the majority of landslide deposits they identified in
218 the region date to between the Late Pleistocene and Holocene. We identify circumstantial evidence
219 which suggests that the Komansu rock avalanche also corresponds to this time with an age of at least
220 several thousand years.

221 The rock avalanche deposit itself has two continuous thrust fault scarps of the MPT running through
222 it (Fig. 2) with 30 m high surface displacements. These scarps represent multiple surface ruptures of
223 the MPT through the deposit since it was emplaced. On major faults such as the MPT, recurrence
224 intervals between major earthquakes are *at least* several hundred years (e.g. Lienkaemper et al. 2012)
225 which suggests a deposit age of several thousand years is required. Using the estimated slip rates
226 along the MPT suggests an age of 2,300-5,000 years. Nonetheless, field mapping during this study
227 identified a new trace of the MPT with tens of metres of slip at the surface, 10 km north of the main
228 MPT trace (Fig. 2). Two traces of the fault requires the 2,300-5,000 year ages to be doubled to ~5 to
229 11 ka if the two traces of the fault both accommodate regional deformation.

230 The lack of surficial exposure of the deposit in its proximal section has two possible explanations
231 relevant to the timing of the event. Either the rock avalanche travelled across a glacier, or it was
232 subsequently eroded or buried by fluvio-glacial deposits. For the rock avalanche to have travelled the
233 first ~15 km of its runout along glacial ice requires it to have occurred at a time when the glaciers
234 were substantially more advanced than at present. Despite the suggested age for the deposit being
235 considerably after the last glacial maximum, the upper age estimate corresponds to a time when the
236 regions glaciers were likely to still be more advanced than today. However, if the deposit age
237 corresponds to the lower estimate then the region's glaciers are likely to have substantially retreated,
238 suggesting runout over glacial ice was minimal. Analysis of the deposit age alone is insufficient to
239 determine whether or not runout over glacial ice occurred however, inspection of the excessive
240 runout length may provide some insight.

241

242 Runout Length

243 Large rock avalanches have apparent coefficient of frictions <0.6, lower than those of smaller
 244 (<10⁶m³) rock avalanches (Hsü, 1975). This reduced coefficient of friction has been correlated with
 245 the ratio of excessive runout length to fall height. Hsü (1975) proposed the relationship:

$$246 \quad L_e = L - H / \tan 32 \quad (1)$$

247 where L_e is the excess travel distance, L is the actual travel distance, H is the fall height, and $\tan 32$
 248 represents the ‘normal’ coefficient of friction of rock on rock (Byerlee, 1978). Applying equation 1
 249 shows that the length of the Komansu deposit was five to six times longer than expected for an event
 250 with normal friction (Table 1). Another measure of excessive runout length, *fahrböschung*, which
 251 measures the angle between the maximum elevation of the pre-event source and the distal extent of
 252 debris, is just 6.1° and is similar to other massive rock avalanche events (Table 2).

Parameter	Value
Debris volume, V (m ³)	10 ¹⁰
Final deposit elevation (m)	2,800
Source zone elevation (m)	5,800
Fall height, H (m)	3,000
Runout length, L (m)	28,000
Excessive runout length, L_e (m)	23,199
Apparent coefficient of friction	0.11
<i>Fahrböschung</i>	6.1°

253 **Table 1 Runout parameters of the Komansu rock avalanche.**

254

255 The excessive runout of the Komansu rock avalanche is emphasised by the fact that for the latter half
 256 of its runout length, after it entered the Alai Valley, it appears to have been unconfined. Nicoletti and
 257 Sorriso-Valvo (1996) analysed 40 rock avalanche deposits in an attempt to find the extent to which
 258 local morphology controls the motion and shape of such events. They distinguished 3 ways in which
 259 morphology affected motion: a) channeling; b) unconfined spreading; and c) right-angle impact of
 260 the debris with mobility reducing from a to c. Nicoletti and Sorriso-Valvo (1996) established
 261 equations to forecast maximum runout lengths in each case for a given volume:

$$262 \quad \text{a) } L = -11.1 + 23.6 \log V \quad (2)$$

$$263 \quad \text{b) } L = -1.22 + 4.66 \log V \quad (3)$$

$$264 \quad \text{c) } L = -4.38 + 5.11 \log V \quad (4)$$

265 where L is in kilometres and V is in millions of km³. Given the Komansu rock avalanche runout was
 266 confined during the first half of its runout and unconfined in the latter half, a maximum runout of

267 between 83 km and 17 km is expected. Similarly Davies (1982) used empirical data to estimate
268 runout lengths compared to volume and found:

$$269 \qquad L = 9.98 V^{0.32} \qquad (5)$$

270 with $r^2 = 0.92$. This suggests an expected runout of >15 km for >10 km³ volume. Runout over glacial
271 ice is therefore not required to explain the long runout of the Komansu rock avalanche.

272

273 Runout Velocity

274 The deposit is present on both banks of the Kyzylsu River (Fig. 2) and appears to have moved uphill
275 as it reached the opposing slope of the Tien Shan. The distal end the deposit is *at least* 100 m higher
276 than its lowest point on the true left bank of the Kyzylsu River. If we assume that the kinetic energy
277 of the rock avalanche was converted completely to gravitational potential energy as it ran uphill upon
278 reaching the Tien Shan, we find the rock avalanche must have been travelling *at least* 45 m s⁻¹ (~160
279 km hr⁻¹) when it reached the Tien Shan. This is a *minimum* estimate of its velocity assuming that all
280 kinetic energy was transferred to potential energy. In reality much of the kinetic energy will be lost
281 to friction, heat, sound etc. A rock avalanche travelling at this velocity, unimpeded, would likely
282 continue to runout for many additional kilometres.

283

284 Runout Mechanism

285 Close inspection of the basal contact in figures 5 and 6 shows that a thin (~10 cm) layer of very fine-
286 grained material separates the rock avalanche deposit from the alluvial deposits (Fig. 8). This
287 material has a consistent fine-sand-to-clay size distribution and distinct upper and lower boundaries
288 (Fig. 8). The ~10 m thick rock avalanche unit above contains large (up to boulder size), angular
289 clasts supported in a fine (up to coarse sand size) matrix. The cause of this stratification of the rock
290 avalanche deposit is likely the result of high normal and shear stresses in the basal region resulting in
291 concentrated comminution of rock debris in this area (Davies et al., 2010).

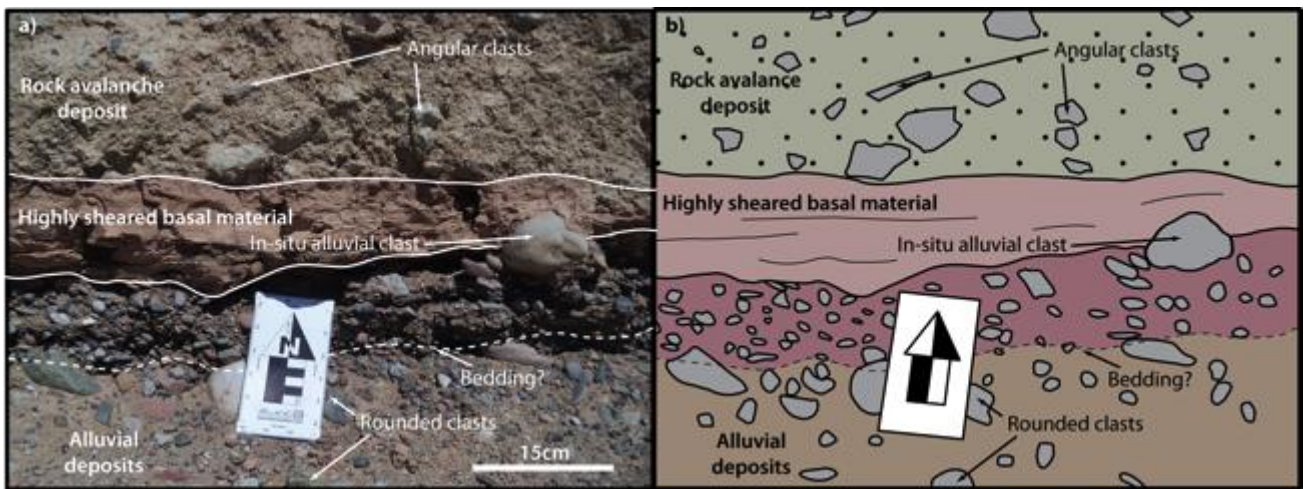
292 Similar stratification has been identified in the Socompa volcanic debris avalanche deposit in Chile
293 (Le Corvec, 2005) which occurred 7,200 yr B.P., had a total volume of 36 km³ (only ~25 km³ was
294 involved in the runout however, with the rest remaining proximal to the volcano), and a runout of 40
295 km (Wadge et al. 1995; Van Wyk de Vries et al., 2001). The Socompa event formed a heavily
296 fragmented lower unit containing thin internal shear bands and an overlying, less fragmented breccia
297 deposit (Wadge et al. 1995; Le Corvec, 2005). Furthermore, the Socompa deposit also has prominent
298 non-striated hummocky topography and an average thickness on the order of 40 m (Davies et al.,
299 2010) and therefore bears notable similarities to the Komansu deposit.

300 The Socompa event was modelled numerically first by Kelfoun and Druitt (2005) using a constant
301 basal shear resistance, then by Davies et al. (2010) who found that the deposit morphology could be
302 sufficiently replicated in the model by applying a basal resistance factor derived from theoretical
303 analysis of rock fragmentation. This provides a mechanical explanation for the small apparent
304 coefficient of friction and the excessive runout lengths of both the Socompa and Komansu events.
305 Davies (1982) estimated the apparent coefficient of friction for various debris volumes from
306 available empirical data; for a deposit with a volume of 10 km^3 the expected apparent coefficient of
307 friction was 0.11. We estimate that the Komansu deposit contains a volume of *at least* 10 km^3 and
308 have shown that the apparent coefficient of friction for the event was ~ 0.11 (Table 1). Wadge et al.
309 (1995) similarly estimated that the Socompa event had a coefficient of friction of 0.07-0.14.

310 The process of dynamic rock fragmentation proposed by Davies et al. (2010) provides a plausible
311 mechanism for the occurrence of this value of basal shear resistance. This suggests that when
312 fragmentation is confined to a basal layer, explosive failure of rock particles exerts a pressure on the
313 overlying material, supporting its weight and reducing the basal effective stress, resistance and thus
314 the apparent coefficient of friction. This mechanism is therefore able to explain the presence of a
315 highly fragmented basal unit, an overlying less fragmented unit, and the reduced basal shear
316 resistance noted in both the Socompa debris avalanche deposit and the Komansu deposit.

317 A final factor that may have influenced the excessive runout is if part of the runout lay over glacial
318 ice. This factor is accepted as typically enhancing runout with a basal friction coefficient of 0.1 (e.g.
319 McSaveney, 1978; Eisbacher, 1979; Evans and Clague, 1988). Such a coefficient corresponds to our
320 calculated value for the Komansu deposit (Table 1) and, combined with the lack of proximal deposit
321 exposure, suggests the possibility that the rock avalanche at least partially ran out across glacier.
322 However, given that the deposit length is similar to other events of this magnitude (Table 2), it is not
323 necessary to infer supraglacial runout.

324



325

326

327

328

329

330

331

332

333

334

335

336

337

338

339

340

341

342

343

344

345

346

347

348

349

350

Fig 8 Interpreted photo (a) and sketch (b) of basal contact between rock avalanche deposit and alluvial deposits. Note the highly sheared material at the base of the rock avalanche deposit which has flowed over the alluvial deposits without moving the large clast at the right of the image. This suggests relatively low basal shear stress as required by the long runout.

Discussion

Size and Runout Length

The Komansu rock avalanche deposit has a maximum straight line distance between the source zone and distal end of ~26 km although we estimate a likely curvilinear runout path of ~28 km (Fig. 2). Maximum width of the deposit is ~11 km; the exposed deposit has a fairly uniform width (Fig. 2). The total exposed deposit covers an area ~120 km² although accounting for the non-exposed deposit suggests it could cover a total area of >250 km². Only a single exposure containing a cross-sectional profile of the deposit has thus far been identified, located at the distal end of the deposit (Figs. 5 & 6). This exposure shows a total deposit thickness of ~10 m and the upper contact has no evidence of erosion. Without further cross-sectional exposures it is difficult to estimate whether this thickness represents a likely maximum or minimum. We note however, for the Socompa rock avalanche the deposit thickness varies between 40 m and 90 m (Wadge et al., 1995) while the (valley-confined) Flims rock avalanche varies greatly, up to a maximum of 500 m (Pollet and Schneider, 2004). We also note that the characteristic hummocks of the Komansu deposit are up to 40 m or more in height suggesting much greater thickness than that visible in outcrop. It therefore seems likely that ~10 m is a minimum thickness and the average is likely to be considerably larger than this. Thus we estimate the Komansu rock avalanche involved a volume of *at least* 10 km³, and probably considerably more. Our minimum estimates suggest that the Komansu rock avalanche is one of the largest subaerial rock avalanches currently identified on Earth. Its estimated volume is comparable to that of the notable Flims rock avalanche in Austria (Pollet and Schneider, 2004) and the Tsergo Ri rock avalanche in

351 Nepal (Schramm et al., 1998; Ibetsberger, 1996) (Table 2). However, depending on its true
 352 thickness, the Komansu rock avalanche may in fact be appreciably larger than both. Only the Bogd
 353 Fault event in Mongolia at 50 km³ (Philip and Ritz, 1999), the Saidmarreh event in Iran at 45 km³
 354 (Roberts and Evans, 2013), and the Socompa event in Chile at 36 km³ (Wadge et al., 1995) contain
 355 larger volumes (Table 2). At 28 km the Komansu runout length is second only to the 40 km runout
 356 Socompa event, being far larger than the 19 km Saidmarreh and 20 km Bogd Fault events despite
 357 both having larger volumes (Table 2). However, the Socompa event was a volcanic debris avalanche,
 358 and these generally appear to involve larger volumes and higher mobility's than non-volcanic rock
 359 avalanches (Dade and Huppert, 1998). Thus the Komansu event represents the largest identified
 360 runout, and likely the third largest volume, of a subaerial, non-volcanic rock avalanche on Earth.
 361

Rock Avalanche	Volume (km³)	Runout length (km)	Friction coefficient
Bogd Fault (Mongolia)	50	20	0.05
Saidmerrah (Iran)	45	19	0.04
Socompa (Chile) ^a	36	40	0.07-0.14
Flims (Austria)	12	16.5	0.12
Komansu (Kyrgyzstan)	>10	28	0.11
Tsergo Ri (Nepal)	10	~12	~0.22
Fernpass (Austria)	1	10.8 & 15.5 ^b	0.11 & 0.09 ^b

362 Table 2 – Comparison of the largest subaerial rock avalanches from around the world. See text for references.

363 ^aVolcanic debris avalanche. ^bDuring runout the Fernpass rock avalanche split into two branches with different
 364 runout lengths and associated friction coefficients.

365

366 Initiation

367 Establishing the trigger for an ancient event such as the Komansu rock avalanche is difficult and
 368 requires a number of assumptions. Nevertheless, a most likely cause can be arrived at by a process of
 369 elimination. This region is especially arid and has likely been so for the majority of the Quaternary
 370 period (e.g. Abramowski et al., 2006), making heavy or long-duration precipitation unlikely.
 371 Furthermore, such rainstorm events rarely result in large, deep-seated rock slope failures such as that
 372 required for the Komansu event, thus we do not consider this a likely cause. Similarly, rapid snow
 373 melt and permafrost degradation are unlikely to result in deep-seated failures. The most likely trigger
 374 is therefore strong ground motions during a large local earthquake. The MPT has been the main
 375 source of tectonic uplift in this region for several million years and was certainly active at the time of
 376 the Komansu rock avalanche. Importantly there are MPT fault scarps up to ~30 m high running

377 through the deposit that represent multiple ruptures along the MPT in the area since the rock
378 avalanche was deposited (Arrowsmith and Stecker, 1999). Furthermore, the MPT is known to be
379 capable of generating large-to-great (M7-8) earthquakes and is sufficiently close to the Trans Alai
380 ranges to generate high intensity shaking in the source region, with substantial topographic
381 amplification in the upper parts of the range (Buech et al., 2010). Historically, large earthquakes are
382 known to have caused sizeable rock avalanches with excessive runouts. The Bogd Fault, Saidmarreh,
383 and Tsergo Ri events are all inferred to have seismic triggers associated with nearby major fault
384 systems (Phillip and Ritz, 1999; Roberts and Evans, 2013; Weidinger et al., 1996). It therefore seems
385 most likely that the Komansu rock avalanche was initiated by a large-to-great (M7-M8) earthquake
386 occurring on the MPT in the central Alai Valley.

387

388 Hazard Analysis

389 The identification of the Komansu rock avalanche presents several important issues for future hazard
390 analysis. Firstly, the re-interpretation of this deposit as a rock avalanche deposit rather than a glacial
391 deposit, combined with several other notable examples globally, suggests that massive landslides are
392 more common than previously thought. Further assessment of other 'glacial deposits' within the Alai
393 Valley is required in order to understand how frequently such events occur in this region. Continued
394 global assessment of deposits such as the Komansu deposit are likely to yield further examples of
395 this misinterpretation. Thus mountainous areas with glacial deposits, particularly those coincident
396 with active faults, are likely to have a much higher rock avalanche hazard than currently believed.

397 The mechanism(s) involved in the excessive runout length are also important. Most towns and
398 villages within the Alai Valley are situated at its northern extent, at the base of the Tien Shan (Fig 1).
399 Prior to identification of the Komansu rock avalanche, the major mass movement hazard posed to
400 these towns and villages was that from the Tien Shan. However, the Komansu rock avalanche
401 suggests that these locations have always had the additional threat of long runout rock avalanches
402 originating in the Trans Alai. Our work demonstrates that the small apparent coefficient of friction
403 that resulted in the large runout length was the result of either runout over glacial ice, or of dynamic
404 fragmentation of rock material in the basal region, or a combination of these. If runout over glacial
405 ice was necessary to explain the deposit extent then the retreat of glaciers in the region would
406 suggest that a recurrence of a similar event is unlikely as future events would have only limited
407 runout length over ice. However, since the runout appears to be satisfactorily explained by dynamic
408 fragmentation, and there is evidence that this process occurred, then a long runout rock avalanche
409 could occur at any time as the only pre-requisite is the failure of a large enough volume of material.
410 Given the potential for a large-magnitude earthquake in the region, the occurrence of a future large-

411 volume rock avalanche with similar runout characteristics cannot be discounted. Conclusively
412 establishing the dominant mechanism involved during runout is therefore vital to better
413 understanding these events and the hazard they pose.

414

415 **Conclusions**

416 Reanalysis of a deposit in the central Alai Valley in southern Kyrgyzstan that was previously thought
417 to be of glacial origin demonstrates that it is instead a massive coseismic rock avalanche deposit.
418 This deposit, on the true right of the Komansu River, covers an area $>250 \text{ km}^2$, contains a volume of
419 at least 10 km^3 and probably considerably more, and has a total runout length of $\sim 28 \text{ km}$. It is thus
420 the longest-runout, and one of the largest-volume, subaerial, non-volcanic rock avalanches thus far
421 identified on Earth. Runout of the debris was halted when it reached the lower slopes of the Tien
422 Shan at the northern boundary of the Alai Valley. Here the debris ran uphill for up to 100 m
423 suggesting it was travelling *at least* 45 ms^{-1} before it stopped. The event appears to have occurred at
424 least 5,000-11,000 years ago, possibly during a time when the regions glaciers were further
425 advanced. The most likely cause was a large-to-great (M7-M8) earthquake centred on the range-
426 bounding Main Pamir Thrust. This fault has a fast slip-rate and is known to have produced
427 earthquakes of this size in recent history. The runout length corresponds to an apparent coefficient of
428 friction of ~ 0.11 , consistent with other events of this size which have not involved runout over ice.
429 This small apparent coefficient of friction may be the result of partial runout over glacial ice;
430 dynamic fragmentation of a thin basal layer; or a combination of both. Runout over glacial ice has
431 been shown to typically result in basal friction coefficients of 0.1, while dynamic fragmentation
432 explains both the observed internal structure of the Komansu deposit and its long runout. Thus the
433 presence of advanced glaciers is not necessary to explain the deposit extent, and such events could
434 recur in the future. Additional mapping, field investigations, and analysis of other glacial landforms
435 in active mountain belts worldwide may assist with the discovery of other large-runout rock
436 avalanches and hazard assessments.

437

438 **Acknowledgements**

439 We thank Dr Kanatbek Abdrakhmatov, Kyrgyzstan Institute of Seismology, for his invaluable field
440 knowledge and support; Ainagul, our cook and Kyrgyz translator; Muhtarbek our driver and minder;
441 Prof. Alexander Strom for his thoughtful discussions; and the Kyrgyz Nomad family who fed us in
442 the field and educated us in Kyrgyz social customs. This research was funded by FRST contract
443 CO5X0402 between GNS Science Ltd and University of Canterbury.

444

445 **References Cited**

- 446 Abramowski U, Bergau, A, Seebach D, Zech R, Glaser B, Sosin P, Kubik PW, Zech W (2006)
447 Pleistocene glaciations of Central Asia: results from ¹⁰Be surface exposure ages of erratic
448 boulders from the Pamir (Tajikistan), and the Alay–Turkestan range (Kyrgyzstan). *Quaternary*
449 *Science Reviews*, 25:1080-1096.
- 450 Arrowsmith JR, Strecker MR (1999) Seismotectonic range-front segmentation and mountain-belt
451 growth in the Pamir-Alai region, Kyrgyzstan (India-Eurasia collision zone). *Geol. Soc. Am.*
452 *Bull.* 111.11:1665-1683.
- 453 Barth NC (2013) The Cascade rock avalanche: implications of a very large Alpine Fault-triggered
454 failure, New Zealand. *Landslides* 1-15. doi: 10.1007/s10346-013-0389-1
- 455 Buech F, Davies TRH, Pettinga JR (2010) The Little Red Hill Seismic Experimental Study:
456 Topographic Effects on Ground Motion at a Bedrock-Dominated Mountain Edifice. *Bull.*
457 *Seismol. Soc. Am.* 100:2219 - 2229.
- 458 Burtman VVS, Molnar PH (1993) Geological and geophysical evidence for deep subduction of
459 continental crust beneath the Pamir (Vol. 281). GSA Bookstore.
- 460 Byerlee J (1978) Friction of rocks. *Pure & Appl. Geophys.* 116.4-5:615-626.
- 461 Coutand I, Strecker MR, Arrowsmith JR, Hilley G, Thiede RC, Korjenkov A, Omuraliev M (2002)
462 Late Cenozoic tectonic development of the intramontane Alai Valley,(Pamir-Tien Shan region,
463 central Asia): An example of intracontinental deformation due to the Indo-Eurasia collision.
464 *Tectonics* 21.6:1053-1072.
- 465 Dade WB, Huppert HE (1998) Long-runout rockfalls. *Geol.* 26.9:803-806.
- 466 Davies TRH (1982) Spreading of rock avalanche debris by mechanical fluidization. *Rock Mech.*
467 15.1:9-24.
- 468 Davies TRH, McSaveney MJ (2012) Mobility of long-runout rock avalanches. In: Clague JJ, Stead
469 D (eds) *Landslides: Types, Mechanisms and Modeling*: Cambridge University Press: 50-
470 58. ISBN-13: 9781107002067
- 471 Davies TRH, McSaveney M, Kelfoun K (2010) Runout of the Socompa volcanic debris avalanche,
472 Chile: a mechanical explanation for low basal shear resistance. *Bull. Volcanol.* 72.8:933-944.
- 473 Dufresne A, Davies TRH, McSaveney MJ (2010) Influence of runout-path material on emplacement
474 of the Round Top rock avalanche, New Zealand. *Earth Surf. Process. Landf.* 35.2:190-201.
- 475 Eisbacher GH (1979) Cliff collapse and rock avalanches (sturzstroms) in the Mackenzie Mountains,
476 northwestern Canada. *Can. Geotech. J.* 16.2:309-334.
- 477 Erismann TH (1979) Mechanisms of large landslides. *Rock Mech.* 12.1:15-46.

478 Evans SG, Clague JJ (1988) Catastrophic rock avalanches in glacial environments. Proceedings of
479 the 5th International Symposium on Landslides 2:1153-1158.

480 Fan G, Ni JF, Wallace TC (1994) Active tectonics of the Pamirs and Karakorum. *J. Geophys. Res.*
481 *Solid Earth* (1978–2012) 99.B4:7131-7160.

482 Hauser A (2002) Rock avalanche and resulting debris flow in Estero Parraguirre and Rio Colorado,
483 Regio'n Metropolitana, Chile. In: Evans SG, DeGraff JV (eds) *Catastrophic landslides: effects,*
484 *occurrence, and mechanisms: Boulder, Colorado, Geological Society of America Reviews in*
485 *Engineering Geology* 15, pp135-148.

486 Hewitt K (1999) Quaternary moraines vs catastrophic rock avalanches in the Karakoram Himalaya,
487 northern Pakistan. *Quaternary Res.* 51.3: 220-237.

488 Howard KA (1973) Lunar avalanches. *Lunar and Planetary Institute Science Conference Abstracts*
489 4:386.

490 Hsü KJ (1975) Catastrophic debris streams (sturzstroms) generated by rockfalls. *Geol. Soc. Am.*
491 *Bull.* 86.1:129-140.

492 Ibetsberger HJ (1996) The Tsergo Ri landslide: an uncommon area of high morphological activity in
493 the Langthang valley, Nepal. *Tectonophysics.* 260:85-93.

494 Krumbiegel C, Schurr B, Orunbaev S, Rui H, Pingren L, TIPAGE Team (2011) The 05/10/2008 Mw
495 6.7 Nura earthquake sequence on the Main Pamir Thrust. *Geophys. Res. Abstr.* 13:4846.

496 Kelfoun K, Druitt TH (2005) Numerical modeling of the emplacement of Socompa rock avalanche,
497 Chile. *J. Geophys. Res. Solid Earth* (1978–2012), 110.B12:1-13. doi:10.1029/2005JB003758

498 Le Corvec N (2005) Socompa volcano destabilisation (Chile) and fragmentation of debris
499 avalanches. MSc thesis, Université Blaise Pascal, Clermont-Ferrand, France, 67p.

500 Lienkaemper JJ, McFarland FS, Simpson RW, Bilham RG, Ponce DA, Boatwright JJ, Caskey SJ
501 (2012) Long-Term Creep Rates on the Hayward Fault: Evidence for Controls on the Size and
502 Frequency of Large Earthquakes. *Bull. Seismol. Soc. Am.* 102.1:31-41.

503 Lucas A, Mangeney A (2007) Mobility and topographic effects for large Valles Marineris landslides
504 on Mars. *Geophys. Res. Lett.* 34.L10201:1-5.

505 Lucchitta BK (1978) A large landslide on Mars. *Geol. Soc. Am. Bull.* 89:1601-1609

506 McColl ST, Davies TRH (2010) Evidence for a rock-avalanche origin for 'The Hillocks' "moraine",
507 Otago, New Zealand. *Geomorphology* 127:216-224

508 McSaveney MJ (1978) Sherman glacier rock avalanche, Alaska, USA. *Rockslides and Avalanches,*
509 1:197-258.

510 McSaveney MJ (2002) Recent rockfalls and rock avalanches in Mount Cook national park, New
511 Zealand. *Catastrophic landslides: effects, occurrence, and mechanisms*, 15:35-70.

512 Melosh HJ (1979) Acoustic fluidization: A new geologic process? *J. Geophys Res. Solid Earth*
513 (1978–2012), 84.B13:7513-7520.

514 Nicoletti PG, Sorriso-Valvo M (1996) Geomorphic controls of the shape and mobility of rock
515 avalanches. *Geol. Soc. Am. Bull.* 103:1365-1373

516 Nikonov AA, Vakov AV, Veselov IA (1983) *Seismotectonics and Earthquakes in the Convergent*
517 *Zone Between the Pamir and Tien Shan (in Russian)*. Nauka, Moscow.

518 Philip H, Ritz JF (1999) Gigantic paleolandslide associated with active faulting along the Bogd fault
519 (Gobi-Altay, Mongolia). *Geol.* 27.3:211-214.

520 Prager C, Krainer K, Seidl V, Chwatal W (2006) Spatial features of holocene sturzstrom-deposits
521 inferred from subsurface investigations (Fernpass rockslide, Tyrol, Austria). *Geo. Alp*, 3:147-
522 166.

523 Pollet N, Schneider JL (2004) Dynamic disintegration processes accompanying transport of the
524 Holocene Flims sturzstrom (Swiss Alps). *Earth Planet. Sci. Lett.* 221.1:433-448.

525 Quantin C, Allemand P, Mangold N, Delacourt C (2004) Ages of Valles Marineris (Mars) landslides
526 and implications for canyon history. *Icarus*, 172.2:555-572.

527 Reznichenko NV, Davies TRH, Shulmeister J, Larsen SH (2012) A new technique for identifying
528 rock avalanche-sourced sediment in moraines and some paleoclimatic implications. *Geol.*
529 40.4:319-322.

530 Reznichenko N, Davies TRH, Robinson TR, De Pascale G (2013) Rock avalanche deposits in Alai
531 Valley, Central Asia: misinterpretation of glacial record. *EGU General Assembly Conference*
532 *Abstracts*, 15:182.

533 Robert NJ, Evans SG (2013) The gigantic Seymareh (Saidmarreh) rock avalanche, Zagros Fold-
534 Thrust Belt, Iran. *J. Geol. Soc.* 170.4:685-700.

535 Schramm JM, Weidinger WE, Ibetsberger HJ (1998) Petrologic and structural controls on
536 geomorphology of prehistoric Tsergo Ri slope failure, Langtang Himal, Nepal. *Geomorph.*
537 26:107-121

538 Shatravin VI (2000) Reconstruction of Pleistocene and Holocene glaciations in Tien-Shan and
539 Pamir: New Results. *Pamir and Tien-Shan: Glacier and Climate Fluctuations during the*
540 *Pleistocene and Holocene: International Workshop*.

541 Shreve RL (1966) Sherman landslide, Alaska. *Science*, 154.3757:1639-1643.

542 Sigurdsson O, Williams Jr RS (1991) Rockslides on the Terminus of Jökulsárgilsjökull, Southern
543 Iceland. *Geogr. Ann. Ser. A. Phys. Geogr.* 129-140.

- 544 Strecker MR, Hilley GE, Arrowsmith JR, Coutand I (2003) Differential structural and geomorphic
545 mountain-front evolution in an active continental collision zone: The northwest Pamir,
546 southern Kyrgyzstan. *Geol. Soc. Am. Bull.* 115.2:166-181.
- 547 Turnbull JM, Davies TRH (2006) A mass movement origin for cirques. *Earth Surf. Process. Landf.*
548 31.9:1129-1148.
- 549 Van Wyk de Vries B, Self S, Francis PW, Keszthelyi L (2001) A gravitational spreading origin for
550 the Socompa debris avalanche. *J. Volcanol. Geotherm. Res.* 105.3:225-247.
- 551 Wadge G, Francis PW, Ramirez CF (1995) The Socompa collapse and avalanche event. *J. Volcanol.*
552 *Geotherm. Res.* 66.1:309-336.
- 553 Weidinger JT, Schramm JM, Surenian R (1996) On preparatory causal factors, initiating the
554 prehistoric Tsergo Ri landslide (Langthang Himal, Nepal). *Tectonophysics* 260:95-107.
- 555 Zubovich AV, Mikolaichuk AV, Kalmetieva ZA, Mosienko OI (2009) Contemporary geodynamics
556 of Nura M=6.6 earthquake area (Pamir-Alai) In: Bulashevich YP (ed) *Fifth Reading:*
557 *Geodynamics, deep structure, heat field of Earth. Geophysical field interpretation (in Russian).*
558 Ekaterinburg.